Journal of Catalysis **203,** 33–40 (2001)
doi:10.1006/jcat.2001.3314, available online at http://www.idealibrary.com on IDEAL®

Theoretical Analysis of Sulfur Exchange Experiments

F. E. Massoth,[1] T. Koltai, and P. Tétényi

Institute of Isotope and Surface Chemistry, Chemical Research Center, Hungarian Academy of Science, P.O. Box 77, H-1525 Budapest, Hungary

Received November 7, 2000; revised June 7, 2001; accepted June 13, 2001; published online August 28, 2001

A flow recirculation, isotopic tracer method was employed to determine sulfur uptake and sulfur exchange for a number of catalysts consisting of combinations of Mo, W, Ni, Co, Pd, and Pt, supported on alumina. By considering adsorption and exchange equilibria, basic equations were derived for calculation of extent of sulfur heteroexchange and fraction of exchangeable sulfur in the sulfided catalysts. Exchange equilibrium was experimentally established by approaching exchange from opposite directions. Variations in sulfur uptake and extent of exchange were obtained for the different catalysts. In all cases, the exchangeable sulfur was less than the total sulfur content. It is proposed that the fraction exchangeable sulfur is related to the edge S to total S ratio of the basic MoS_2 particles. On this basis, average MoS_2 slab sizes were estimated by application of slab models. The amount of exchangeable sulfur correlated reasonably well with thiophene hydrodesulfurization activity of the catalysts. © 2001 Academic Press

Key Words: **^{35}S; Mo; CoMo; NiMo; NiW; PdMo; PtMo; S exchange; S uptake; thiophene HDS.**

INTRODUCTION

Many exchange studies have utilized tracers, mostly radioactive $H_2{}^{35}S$, to gain insight into the amount of "labile" (exchangeable) sulfur species on supported sulfide catalysts, as well as the relation between these species and hydrodesulfurization (HDS) activity. In most of the studies, the extent of sulfur exchange was less than the total catalyst sulfur content and increased with temperature. Scarpiello *et al.* (1) showed that only 30% of the sulfur content of a Mo/Al_2O_3 catalyst was exchanged at 400°C and that the same catalyst with added nickel exhibited about twice the amount of exchangeable sulfur. A limiting extent of sulfur exchange of about 40% above about 400°C was found by Massoth and Zeuthen (2) for a Mo/Al_2O_3. Kabe and coworkers (3, 4) showed that the ratio of labile sulfur to total sulfur was less than 50% for a $CoMo/Al_2O_3$ catalyst and that the HDS activity was related to the extent of the exchange sulfur. A linear relationship between amount of mobile sulfur and HDS activity for several $CoMo/Al_2O_3$ catalysts was demonstrated by Kogan *et al.* (5). In the above studies the HDS activity was evaluated using thiophene. Qian *et al.* (6) found a correlation between the product of the amount and the rate of sulfur exchange versus the HDS activity of dibenzothiophene. In contrast, Startsev *et al.* (7) reported that the rate HDS of thiophene was unrelated to the sulfur mobility (rate of exchange) for Mo/SiO_2 and $NiMo/SiO_2$ catalysts. In all these cases, the studies involved only one or two similar catalyst systems. Thus, the findings were limited in scope.

In a previous paper, we outlined a newly developed radioactive tracer method employing a recirculation system for the determination of sulfur uptake capacity and of sulfur heteroexchange between catalyst and gas phase H_2S (8). The sulfur uptake and exchange values in that study were calculated in a simplified way—changes in adsorption/desorption with partial pressure of H_2S and reverse exchange were neglected. This simplified method has been applied to several Mo-based alumina supported catalysts (8–10). Data for two differently prepared $NiMo/Al_2O_3$ catalysts gave indications of a relationship between sulfur exchange and HDS activity (9).

Here we undertake a theoretical analysis of the sulfur uptake and exchange experiments and demonstrate the validity of the method. The uptake capacity and extent of exchange are calculated from data published previously for a number of Mo-based alumina-supported catalysts. In addition, exchange experiments are performed and analyzed on several new catalysts. Sulfur uptake and exchange for seven different catalyst systems are compared to their thiophene HDS activities.

THEORY

A brief outline of the experiments involved in the radioactivity exchange studies accompanies development of the theory. More details on radioactivity measurements and procedures are given in the Experimental section and in a previous paper (8).

---

[1] To whom correspondence should be addressed. Department of Chemical and Fuels Engineering, University of Utah, 50 S. Central Campus Drive, Room 3290, Salt Lake City, Utah 84112-9203.

0021-9517/01 $35.00

Two schemes are performed, comprising several steps in which radioactivity measurements are made. The following assumptions are made:

1. The ratio of radioactive to nonradioactive H_2S in the starting gas mixture is the same in all steps, except steps 3 and 4, in which nonradioactive H_2S/H_2 of the same total amount of H_2S is used.
2. The catalyst sulfur, S^{cat} (formally S^{irr} in (8)), is in equilibrium with the gas phase at end of each step.
3. The adsorbed H_2S, S^{ad} (formally S^{rev}), is in equilibrium with the gas phase at end of each step.
4. Only a fraction of the S^{cat} is exchangeable.

Scheme A

Step 1. In this step, the catalyst in oxide form is sulfided by circulating over the catalyst a mixture of $H_2{}^*S$ ($^*S$ refers to radioactive ^{35}S) and H_2S (S refers to ^{32}S) in H_2, and the residual radioactivity of the $H_2{}^*S$ remaining in the gas phase is measured until no further change. This process converts metal oxides to their sulfides and leaves adsorbed sulfur species on the catalyst surface.

At initial conditions, the total H_2S partial pressure is given by p_{so}, and the total amount of H_2S by m_{so}. Let $^*m_{so}$ be the initial moles of $H_2{}^*S$ in the mixture (not actually known), and let R be the ratio of $H_2S/H_2{}^*S$ ($\sim 10^{12}$). Then the moles of $H_2{}^*S$ lost in the gas phase, $^*Y_1$, is

$$^*Y_1 = {}^*m_{so}(1 - I_1/I_o) = {}^*S_{1T}, \qquad [1]$$

where I_1 is the radioactivity in the gas phase at line out, I_o is the radioactivity of the initial mixture, and $^*S_{1T}$ is the total radioactive sulfur uptake. The latter consists of irreversibly bonded sulfur, e.g., metal sulfide formed, $^*S_1^{cat}$, and reversibly attached (presumably adsorbed) sulfur species, $^*S_1^{ad}$ ($H_2{}^*S$ or $^*SH$). If we assume no kinetic isotope effect, the ratio of $S_{1T}/{}^*S_{1T}$ (also $S_1^{cat}/{}^*S_1^{cat}$ and $S_1^{ad}/{}^*S_1^{ad}$) should be the same as that in the gas phase, which ratio should not change during the run. Then, since $^*m_{so} = m_{so}/R$, where m_{so} is the measured total H_2S in the gas phase at start of run, we have

$$Y_1 = R^*Y_1 = m_{so}(1 - I_1/I_o) = S_{1T}, \qquad [2]$$

where Y_1 is the total S uptake based on initial moles of H_2S present, and S_{1T} consists of S_1^{cat} plus S_1^{ad} (both include $^*S_1^{cat}$ and $^*S_1^{ad}$). Hence,

$$^*Y_1 = {}^*S_1^{cat} + {}^*S_1^{ad}(\text{at } p_{s1}) \qquad [3]$$

$$Y_1 = S_1^{cat} + S_1^{ad}(\text{at } p_{s1}), \qquad [4]$$

where p_{s1} is the final H_2S partial pressure. The total amount of H_2S left and partial pressure in the final gas phase are given by

$$m_{s1} = m_{so} - Y_1 \qquad [5]$$

$$p_{s1} = p_{so}\ (m_{s1}/m_{so}). \qquad [6]$$

Next, the catalyst is subjected to an evacuation treatment in vacuo for 2 h to remove the adsorbed S species. The catalyst at this stage contains only $^*S_1^{cat}$ and S_1^{cat}.

Step 2. In this step, the catalyst from the previous run is subjected to the identical gas mixture as for Step 1. Since the ratio of R in the gas phase is the same, no net exchange of radioactivity occurs, as $S_1^{cat}/{}^*S_1^{cat}$ is also equal to R and the net result is only adsorption of $H_2{}^*S$ and H_2S. Therefore, as before, the amount of H_2S adsorbed, Y_2, is

$$Y_2 = m_{so}(1 - I_2/I_o) = S_2^{ad}(\text{at } p_{s2}), \qquad [7]$$

where I_2 is the measured reactivity at line out. As before,

$$m_{s2} = m_{so} - Y_2 \quad \text{and} \quad p_{s2} = p_{so}(m_{s2}/m_{so}). \qquad [8]$$

It is now possible to determine S_1^{cat}. However, this cannot be done by directly subtracting Y_2 from Y_1 because of different final partial pressures of H_2S in the two cases, leading to different amounts adsorbed. In fact, $p_{s2} < p_{s1}$, since only adsorption is involved in Step 2, whereas both adsorption and consumption of H_2S due to S^{cat} formation are involved in Step 1. In order to calculate S^{cat} from Eq. [4], it is necessary to correct the amount of adsorption obtained at p_{s2} to that of p_{s1}. This can be done by resort to an isotherm relating the amount of adsorption, Y_2, with H_2S partial pressure, p_{s2}. Then

$$m_{s1} = f(m_{so}, p_{s1}, p_{s2}) \qquad [9]$$

and the corrected Y_2, $^cY_2$, is

$$^cY_2 = f(Y_2, m_{s1}, m_{s2}). \qquad [10]$$

Hence, S_1^{cat} is given by

$$S_1^{cat} = Y_1 - {}^cY_2. \qquad [11]$$

At the end of the run, the catalyst is again evacuated to remove adsorbed H_2S.

Step 3. In this step, nonradioactive H_2S (at the same m_{so} and p_{so}) is passed over the catalyst from Step 2, and the resulting $H_2{}^*S$ evolved from exchange with S^{cat} is determined, measuring gas-phase radioactivity, I_3. Consider the exchange reaction,

$$^*S^{cat} + H_2S \leftrightarrows S^{cat} + H_2{}^*S, \qquad [12]$$

in which there is a net transfer of $^*S_1^{cat}$ to S_1^{cat}. Let X_3 (formally S^{exc}) designate the extent of exchange of sulfur species. Then for every mole transferred, one mole of $^*S^{cat}$ is lost and one mole of S^{cat} is gained; likewise, one mole of H_2S is lost from the gas phase and one mole of $H_2{}^*S$ is gained. The $H_2{}^*S$ formed then begins to participate in the reverse reaction. Both forward and back reactions will continue until equilibrium is achieved, at which point the rates will be the same and no further net change will occur. Thus,

$$^{*}\mathrm{S}_3^{\mathrm{cat}} = {}^{*}\mathrm{S}_1^{\mathrm{cat}} - X_3 \quad \text{and} \quad \mathrm{S}_3^{\mathrm{cat}} = \mathrm{S}_1^{\mathrm{cat}} + X_3. \qquad [13]$$

But X_3 is very small since exchange cannot proceed beyond equilibrium, and only a small amount of $^{*}\mathrm{S}_1^{\mathrm{cat}}$ is present (for large R) to react. Since $\mathrm{S}_1^{\mathrm{cat}} \gg {}^{*}\mathrm{S}_1^{\mathrm{cat}}$, $X_3 \ll \mathrm{S}_1^{\mathrm{cat}}$, and $X_3 \ll \mathrm{S}_3^{\mathrm{cat}}$, then $\mathrm{S}_3^{\mathrm{cat}} = \mathrm{S}_1^{\mathrm{cat}}$.

Exchange equilibrium. Assuming exchange to be at equilibrium, the equilibrium constant for Eq. [12], K^{exc}, is given by

$$\begin{aligned} K^{\mathrm{exc}} &= \left(\mathrm{S}_3^{\mathrm{cat}}\, {}^{*}p_{\mathrm{s}3}\right)/\left({}^{*}\mathrm{S}_3^{\mathrm{cat}}\, p_{\mathrm{s}3}\right) \\ &= \left(\mathrm{S}_3^{\mathrm{cat}}\, {}^{*}m_{\mathrm{s}3}\right)/\left({}^{*}\mathrm{S}_3^{\mathrm{cat}}\, m_{\mathrm{s}3}\right) = k_1/k_{-1}, \qquad [14] \end{aligned}$$

where k_1 and k_{-1} are the rate constants for the forward and back reactions. For no kinetic isotope effect, $k_1 = k_{-1}$, and thus

$$^{*}m_{\mathrm{s}3}/m_{\mathrm{s}3} = {}^{*}\mathrm{S}_3^{\mathrm{cat}}/\mathrm{S}_3^{\mathrm{cat}}. \qquad [15]$$

Now let g_3 be the fraction of $\mathrm{S}_1^{\mathrm{cat}}$ sulfur which is actually exchangeable. Then

$$^{*}\mathrm{S}_3^{\mathrm{cat}}/\mathrm{S}_3^{\mathrm{cat}} = \left(g_3\, {}^{*}\mathrm{S}_1^{\mathrm{cat}} - X_3\right)/g_3\mathrm{S}_1^{\mathrm{cat}}. \qquad [16]$$

From before, $\mathrm{S}_1^{\mathrm{cat}} = Y_1 - {}^{\mathrm{c}}Y_2$, and $^{*}\mathrm{S}_1^{\mathrm{cat}} = \mathrm{S}_1^{\mathrm{cat}}/R$, substitution gives

$$\frac{^{*}\mathrm{S}_3^{\mathrm{cat}}}{\mathrm{S}_3^{\mathrm{cat}}} = \frac{Y_1 - {}^{\mathrm{c}}Y_2 - (R/g_3)X_3}{R(Y_1 - {}^{\mathrm{c}}Y_2)}. \qquad [17]$$

Adsorption equilibrium. Assuming equilibrium adsorption between gas phase and adsorbed species and no kinetic isotope effect gives, similar to above

$$^{*}m_{\mathrm{s}3}/m_{\mathrm{s}3} = {}^{*}\mathrm{S}_3^{\mathrm{ad}}/\mathrm{S}_3^{\mathrm{ad}}. \qquad [18]$$

Since the final H_2S partial pressure is the same as for Step 2, $\mathrm{S}_3^{\mathrm{ad}} = \mathrm{S}_2^{\mathrm{ad}} = Y_2$.

The moles of $H_2{}^{*}S$ in the gas phase, $^{*}m_{\mathrm{s}3} = {}^{*}Y_3$, is a result of exchange and adsorption, viz.

$$^{*}Y_3 = X_3 - {}^{*}\mathrm{S}_3^{\mathrm{ad}} \quad \text{or} \quad {}^{*}\mathrm{S}_3^{\mathrm{ad}} = X_3 - {}^{*}Y_3. \qquad [19]$$

It is also related to the measured radioactivity, I_3, by

$$^{*}Y_3 = {}^{*}m_{\mathrm{so}}(I_3/I_{\mathrm{o}}). \qquad [20]$$

(Note that althought the actual amount of $H_2{}^{*}S$ in the gas mixture at the start of run is zero, the $^{*}m_{\mathrm{so}}$ value in the original standard mixture must be used to obtain the moles of $H_2{}^{*}S$ in the final mixture.) Since $^{*}Y_3$ cannot be determined ($^{*}m_{\mathrm{so}}$ not known), we define Y_3 by

$$Y_3 = m_{\mathrm{so}}(I_3/I_{\mathrm{o}}) = R^{*}Y_3. \qquad [21]$$

Substituting these values yields

$$\frac{^{*}\mathrm{S}_3^{\mathrm{ad}}}{\mathrm{S}_3^{\mathrm{ad}}} = \frac{X_3 - Y_3/R}{Y_2}. \qquad [22]$$

Gas phase mole balance. At equilibrium, the moles of H_2S left in the gas phase is the difference between the starting amount and that adsorbed, since no net change occurs due to exchange. Thus, $m_{\mathrm{s}3} = m_{\mathrm{so}} - \mathrm{S}_3^{\mathrm{ad}}$, and from before, $^{*}m_{\mathrm{s}3} = {}^{*}Y_3 = Y_3/R$, gives

$$\frac{^{*}m_{\mathrm{s}3}}{m_{\mathrm{s}3}} = \frac{Y_3}{R(m_{\mathrm{so}} - Y_2)}. \qquad [23]$$

Combining the latter with the Eqs. [15], [17], [18], and [22] gives the following

$$(R/g_3)X_3 = \frac{\left(Y_1 - {}^{\mathrm{c}}Y_2\right)(m_{\mathrm{so}} - Y_2 - Y_3)}{m_{\mathrm{so}} - Y_2} \qquad [24]$$

$$RX_3 = \frac{m_{\mathrm{so}}Y_3}{m_{\mathrm{so}} - Y_2} \qquad [25]$$

and from Eqs. [24] and [25],

$$g_3 = \frac{m_{\mathrm{so}}Y_3}{\left(Y_1 - {}^{\mathrm{c}}Y_2\right)(m_{\mathrm{so}} - Y_2 - Y_3)}. \qquad [26]$$

Then the total exchangeable sulfur, $X_{\mathrm{T}3} = g_3\, \mathrm{S}_1^{\mathrm{cat}}$, is from Eq. [11]

$$X_{\mathrm{T}3} = \frac{m_{\mathrm{so}}Y_3}{(m_{\mathrm{so}} - Y_2 - Y_3)}. \qquad [27]$$

(It follows from Eq. [27], that the true amount of exchangeable sulfur differs from Y_3, calculated from Eq. [21], applied in previous studies as exchangeable sulfur. The extent of the difference depends on the difference between m_{so} and the sum of $Y_2 + Y_3$. For large m_{so}, $m_{\mathrm{so}} \gg Y_2 + Y_3$, and $X_{\mathrm{T}3} \sim Y_3$.)

Scheme B

Step 4. In this step, another sample of the same oxide catalyst is sulfided with nonradioactive H_2S in H_2 under the same conditions as for Run 1. Following evacuation, the sulfided sample is then reacted with the original $H_2S/H_2{}^{*}S$ in H_2 mixture of Step 1. The residual radioactivity is monitored until no further change occurs. The object of this run is to establish that equilibrium is truly achieved in Step 3 by approaching equilibrium from the opposite direction.

In the first part of the run and after evacuation, only $\mathrm{S}^{\mathrm{cat}}$ is present, no $^{*}\mathrm{S}^{\mathrm{cat}}$. At the end of the second part of the experiment, the catalyst contains $\mathrm{S}_4^{\mathrm{cat}}$, $^{*}\mathrm{S}_4^{\mathrm{cat}}$, $\mathrm{S}_4^{\mathrm{ad}}$, and $^{*}\mathrm{S}_4^{\mathrm{ad}}$.

Assuming exchange and adsorption equilibria are established, we have as for Run 3

$$^{*}m_{\mathrm{s}4}/m_{\mathrm{s}4} = {}^{*}\mathrm{S}_4^{\mathrm{cat}}/\mathrm{S}_4^{\mathrm{cat}} = {}^{*}\mathrm{S}_4^{\mathrm{ad}}/\mathrm{S}_4^{\mathrm{ad}}. \qquad [28]$$

Since there is no ${}^{*}S_4^{cat}$ at start of the second part of the run, all that is formed is due to exchange. Therefore, ${}^{*}S_4^{cat} = X_4$, and from analogy to Eq. [16], leads to

$$\frac{{}^{*}S_4^{cat}}{S_4^{cat}} = \frac{X_4}{g_4 S_1^{cat}} = \frac{X_4}{g_4\left(Y_1 - {}^{c}Y_2\right)}. \qquad [29]$$

Based on total H_2S,

$$Y_4 = m_{so}\,(1 - I_4/I_o) = R\,{}^{*}Y_4 \qquad [30]$$

$${}^{*}Y_4 = X_4 + {}^{*}S_4^{ad}, \qquad [31]$$

where I_4 is the measured reactivity at end of run. Since no net change in total H_2S occurs for exchange, the only loss of H_2S and consequent pressure drop is due to adsorption, identical to Step 2. Thus, $p_{s4} = p_{s2}$, and $S_4^{ad} = S_2^{ad} = Y_2$. Substituting these relations gives

$$\frac{{}^{*}S_4^{ad}}{S_4^{ad}} = \frac{{}^{*}Y_4 - X_4}{Y_2} = \frac{Y_4 - RX_4}{RY_2}. \qquad [32]$$

For the gas phase mole balance

$${}^{*}m_{s4} = {}^{*}m_{so}(I_4/I_o) = (m_{so} - Y_4)/R \qquad [33]$$

$$m_{s4} = m_{so} - S_4^{ad} = m_{so} - Y_2 \qquad [34]$$

$$\frac{{}^{*}m_{s4}}{m_{s4}} = \frac{m_{so} - Y_4}{R(m_{so} - Y_2)}. \qquad [35]$$

Combining the Eq. [35] with Eqs. [28], [29], and [32] yields

$$(R/g_4)X_4 = \frac{(m_{so} - Y_4)\left(Y_1 - {}^{c}Y_2\right)}{m_{so} - Y_2} \qquad [36]$$

$$RX_4 = \frac{m_{so}(Y_4 - Y_2)}{m_{so} - Y_2} \qquad [37]$$

and from Eqs. [36] and [37]

$$g_4 = \frac{m_{so}(Y_4 - Y_2)}{(m_{so} - Y_4)\left(Y_1 - {}^{c}Y_2\right)}. \qquad [38]$$

As before, the total exchangeable sulfur, $X_{T4} = g_4\,S_1^{cat}$, is

$$X_{T4} = \frac{m_{so}(Y_4 - Y_2)}{(m_{so} - Y_4)}. \qquad [39]$$

In summary, Eqs. [26] and [27] allow determination of the fraction of S^{cat} exchanged (g_3) and the total exchangeable S^{cat} (X_{T3}) from data obtained in Steps 1, 2, and 3. Likewise, use of Eqs. [38] and [39] allows calculation of g_4 and X_{T4} from data of Steps 1, 2, and 4. If equilibrium is truly achieved in all runs, these values should be the same, within experimental error.

EXPERIMENTAL

Mo/Al_2O_3 (Mo), $CoMo/Al_2O_3$ (CoMo), and $NiMo/Al_2O_3$ (NiMo) catalysts were prepared in the Chemical and Fuels Engineering Department, University of Utah, by impregnation of a commercial Al_2O_3 (180 m^2/g) with an aqueous solution of ammonium paramolybdate. The wet sample was dried, then calcined overnight at 773 K, to give the Mo catalyst. The CoMo and NiMo catalysts were prepared by impregnation of the dried (not calcined) Mo sample with aqueous cobalt nitrate or nickel nitrate solution, dried and calcined overnight at 773 K. The metal content of the samples was determined by Prompt Gamma Activation Analysis, and their BET surface area by N_2 adsorption. Properties of these catalysts, together with those used in this study and previously reported, are given in Table 1.

The gas recirculation system has been described previously (8). The amounts of uptake and exchange were determined by gas-phase radioactivity measurements of $H_2{}^{35}S$ in a flow-through Eu-doped scintillation radioactivity detector. Details of the radioactivity measurements are given elsewhere (11). The catalyst sample in the reactor vessel, after evacuation, was subjected to either $(H_2{}^{35}S + H_2S)/H_2$ or H_2S/H_2 mixtures at about 53 kPa total pressure, either ~4 or ~27 kPa H_2S partial pressure, and 673 K. The mixtures were circulated through the catalyst until a constant gas-phase radioactivity was reached, usually

TABLE 1

Characteristic Data of the Catalysts

Catalyst (Ref.)[a]	n_{M1}[b] (10^{17} atom/mg)	n_{M2}[c] (10^{17} atom/mg)	Surface area (m^2/g)	HDS (10^{17} molec/s-mg)
Mo	—	5.30	101	2.01
CoMo	3.06	5.03	119	3.10
NiMo	3.03	5.08	117	2.75
NiW-1 (11)	1.43	4.18	313	1.24
NiW-2 (11)	1.52	4.31	361	1.33
PdMo (10)	1.46	4.28	133	1.09
PtMo (10)	0.93	4.99	142	1.54

[a] All catalysts supported on Al_2O_3, except for NiW-2 on SiO_2-Al_2O_3.

[b] Promotor atoms.

[c] Mo or W.

within 2 h. The radioactivity I values were measured in cpm, corrected for background radioactivity, and the respective Y values were calculated from Eqs. [2], [7], [21], and [30]. The errors were ±10% for Y_1, Y_2, and Y_4, and 10–15% for Y_3, corresponding to about 15–20% relative error in the S, g, and X values.

Several separate samples after evacuation at the end of Step 1 were treated in H_2 for 2 h with circulation at ~53 kPa and 673 K. No radioactivity appeared in the gas phase under this treatment, indicating the stability of the sulfide phase at this point. These samples were not subjected to any subsequent steps, and therefore are not included in the S-exchange data.

For the HDS activities, the catalysts were pretreated in a H_2S/H_2 stream (30 NTP cm^3/min, 0.1% H_2S) up to 673 K and holding temperature for 2 h. It was demonstrated that these conditions gave approximately the same catalyst sulfur content as in the S-exchange experiments (12). At the end of the pretreatment period, 5×10^{-4} cm^3 liquid thiophene pulses were injected into a H_2 stream of 30 NTP cm^3/min flow rate, and the products of conversion were analyzed by a GLC column, packed with 18% squalane on Chromosorb P and connected directly downstream of the reactor. Products of reaction were mostly H_2S, butenes, and butane. The degree of thiophene conversion was calculated from the peak areas, corrected for their chromatographic factors. The mean error of three duplicate measurements was about 7%.

RESULTS AND DISCUSSION

Table 2 presents basic data obtained in the exchange experiments performed on the catalysts. Although 12 runs are listed, some consisted of two individual runs under the same conditions, in which one involved measurements of Y_1, Y_2, and Y_3 (Scheme A), and the other Y_4 (Scheme B), resulting in 20 individual runs. In a few runs, Y_2 was not measured. Assuming equilibrium, combination of Eqs. [25] and [37] for $RX_3 = RX_4$, yields $Y_2 = Y_4 - Y_3$. The latter expression was used to calculate Y_2. In these cases, only X_{T3} or X_{T4} could be separately evaluated, as they give the same value.

Values of Y_2 represent the reversible sulfur uptake of adsorbed H_2S. Comparison of Y_2 values with catalyst surface areas of Table 1 show that adsorption is not related to surface area, but must take place on the metal sulfide phases of the catalyst. This was verified by a very low S uptake obtained on a similar support (11). In some cases, especially at the higher H_2S partial pressures, adsorption values exceeded those of catalyst sulfur, indicating that some physical adsorption as well as chemisorption was present.

Corrections to the Y_2 values were necessary, as described in the Theory section. Figure 1 shows equilibrium isotherm data (Y_2 vs p_2) previously reported (8) for another catalyst (CoMo-1). Isotherms for the catalysts in the current study were not obtained, only values at one or two pressures, some of which are included in Fig. 1. It may be assumed that the latter follow the general trend of the CoMo-1 catalyst. It is evident, that at the higher pressure, all catalysts are near to saturation adsorption, consequently, no correction to Y_2 was needed. At low pressure, however, changes in equilibrium pressure between Steps 1 and 2 ($p_{s1} < p_{s2}$) can lead to an appreciable correction to Y_2. At the low pressures involved in these runs and from the apparent curvature of the isotherm for CoMo-1 (Fig. 1), a correction consisting of one-half of the sum of a linear plot of the point $\{Y_2, p_2\}$ through the origin plus no correction seemed best. This

TABLE 2

Basic and Calculated Data for Exchange Experiments

	Run number											
	1	2	3	4	5	6	7	8	9	10	11	12
	Catalyst											
	Mo	Mo	CoMo	NiMo	NiW-1	NiW-1	NiW-2	NiW-2	PdMo	PdMo	PtMo	PtMo
p_{so}	4.04	27.2	4	4.04	4.27	25.8	3.79	26.5	4.02	26.4	3.96	26.9
m_{so}	30.6	207.2	30.3	31.5	28.6	195.6	28.1	195	29.8	203.7	30.2	199.3
Y_1	8.76	12.14	19.29	24.06	10.01	12.47	11.39	13.97	13.87	14.98	10.49	12.64
Y_2	4.17	7.15	7.96	9.94[a]	5.51	7.74	4.71[a]	6.97	5.1[a]	7.68	5.25[a]	7.13
Y_3	2.53	2.62	3.52	3.42	0.69	—	0.84	—	1.24	1.37	0.85	0.83
Y_4	6.87	9.68	11.57	13.36	—	8.43	5.55	7.81	6.34	—	6.10	7.92
${}^{c}Y_2$	3.81	7.06	7.96	9.94	4.97	7.74	4.04	6.97	4.19	7.68	4.70	7.13
S^{cat}	4.95	5.08	11.33	14.03	5.04	4.73	7.35	7.00	9.68	7.30	5.79	5.51
%Sulf.	47	48	86	106	51	48	72	69	97	73	61	58
g_3	0.65	0.54	0.50	0.42	0.17	—	0.14	—	0.16	0.20	0.18	0.16
X_{T3}	3.24	2.75	5.67	5.94	0.88	—	1.05	—	1.58	1.43	1.07	0.86
g_4	0.7	0.52	0.52	—	—	0.15	—	0.13	—	—	—	0.15
X_{T4}	3.48	2.65	5.84	—	—	0.72	—	0.88	—	—	—	0.82

[a] Calculated from Y_4–Y_3. Units: p in kPa; m, Y, S, X in 10^{17} S atoms/mg.

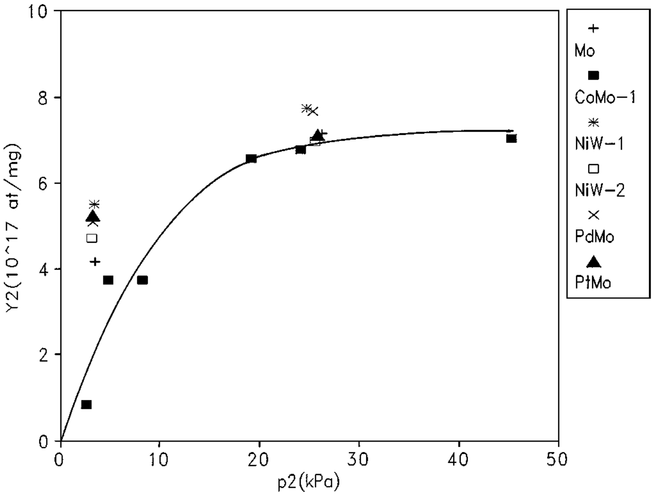

FIG. 1. Isotherm data of adsorption (Y_2) vs H_2S partial pressure (p_2) for a number of catalysts.

correction affects the values of S^{cat} (Eq. [11]) and g (Eqs. [26] and [38]), but not X_T (Eqs. [27] and [39]). The correction was not made for CoMo and NiMo because of their relatively high adsorptions, indicative of near to equilibrium adsorption.

The actual amount of radioactive sulfur exchanged in Step 3 or Step 4 cannot be determined because the actual amount of $H_2{}^{35}S$ in the mixture is not known. However, although undetected, nonradioactive H_2S in the mixture also undergoes exchange with nonradioactive sulfur, which allows determination of the total exchangeable sulfur, X_T, from Eq. [27] or [39]. In addition, the fraction of exchangeable sulfur, g (ratio of exchanged sulfur to total sulfur), can be determined by Eq. [26] or [38]. Since the ratio of $H_2S/H_2{}^{35}S$ was the same in all experiments, at equilibrium, the values of X_{T3} and X_{T4} should be the same, as should g_3 and g_4 for a given catalyst.

Equilibrium in the exchange experiments was demonstrated by approach to exchange from opposite directions, viz. Step 3 vs Step 4, as determined in runs under nearly identical conditions, where values of g_3 and g_4 were essentially the same, as were values of X_{T3} and X_{T4}. Also, values of g and X_T were mostly independent of initial run pressure.

It is seen from Table 2 that in all cases the total exchanged sulfur, X_T, was less than the catalyst sulfur, S^{cat}, in agreement with the literature. Although X_T generally increased with S^{cat}, there is no direct correlation between them.

The sulfur content of the catalysts, S^{cat}, depends on the amount of metals present and on their degree of sulfiding under the experimental conditions employed. The sulfidation procedure adopted was identical for all catalysts, as the aim of this study was to compare the catalysts activity with their sulfur uptake and exchange capacity under the same conditions, even though these may not be optimal for all catalysts. The values of S^{cat} obtained by the radioactivity measurements in this study for the Mo and NiW catalysts are in good agreement with XPS data on the same catalysts (10, 13). A better measure of the degree of the sulfiding is %Sulf., in which S^{cat} is normalized to the common state of the respective sulfides based on complete sulfiding, assuming MoS_2, WS_2, Co_9S_8, NiS, and PdS and PtS. As seen in Table 2, considerable variations in %Sulf. are observed for the different catalysts. The low %Sulf. values for most catalysts are due to the relatively mild sulfiding conditions employed. This indicates that only a portion of the MoO_3 in the oxide state undergoes sulfiding. This was confirmed in the cases of the Mo, PdMo, and PtMo catalysts, where XPS results (10) revealed about 55% of the Mo as Mo(IV), i.e., a high ratio of unconverted MoO_3 present in the sulfided catalysts.

In well-prepared catalysts, sulfided catalysts of Mo (W) consist of stacks of two-dimensional slabs containing the metal atoms sandwiched between two layers of S atoms (14). The edges of the slabs contain S atoms and vacancies (S uncoordinated sites), as well as attached Co (Ni) atoms. Our studies, in agreement with those in the literature, indicated the sulfur exchanged to be less than the total sulfur. This has been interpreted in terms of metal-S bond strengths (7), viz. the edge S atoms are held more weakly than the top S atoms of the slab. For the temperature of this study, it is believed that most, if not all, of the edge S atoms are exchanged (2). The fraction exchangeable sulfur, g, would then represent the ratio of edge S to total S atoms. A higher value of g would indicate a smaller average slab size. The total sulfur exchanged, X_T, will then depend on the fractional exchange and the total S content (Eq. [27] or [39]).

In order to determine if the assumption that g represents the S edge/S total ratio is reasonable, we have compared estimated slab sizes with values found in the literature as determined by extended X-ray absorption fine structure (EXAFS) and transmission electron microcopy (TEM). Using hexagonal (hex) and rhombohedral (rhomb) models of Kasztelan *et al.* (15), the values of Table 3 were obtained. These are based on a basic slab of MoS_2, for an S–S distance of 3.2 nm. For well-prepared Mo/Al_2O_3 catalysts, values of lateral slab sizes of 1.0–1.5 nm were found from EXAFS studies (16, 17), while values some two- to four-times these were reported in TEM studies (18–21). Topsøe *et al.* (14) and Shimada *et al.* (22) explained the difference as being due to the failure of the TEM to detect very small particles, and possible dislocations in the larger slabs. In fact, Eijsbouts *et al.* (23) deduced that only a small fraction of the MoS_2 is detected in TEM photographs. It is noted that Bouwens *et al.* (24) concluded that a large fraction of MoS_2 occurs in units of less that 7 Mo per slab. The g value of 0.5 for our Mo(Run 2) catalyst predicts, according to Table 3, a size of ∼1.3 nm, in good agreement with the EXAFS results. The higher g value for the Mo(Run 1) catalyst, 0.65, is not consistent with either a hex or rhomb slab model. However, Lauritsen *et al.* (25) have recently demonstrated that a stable triangular slab is possible for MoS_2. Calculations indicate that a g of 0.65 nm, would represent a triangular

TABLE 3

Relation between S edge (S_e)/S total (S_T) and Length (L) for MoS_2 Slabs

n_1	n_2	Mo	S_T	S_e	S_e/S_T	L_{max}, nm
			Hex			
2	3	8	16	8	0.50	1.3
3	3	12	24	10	0.42	1.6
3	4	21	42	14	0.33	1.9
4	4	27	54	16	0.30	2.2
4	5	40	80	20	0.25	2.6
5	5	48	96	22	0.23	2.9
			Rhomb			
4	4	9	18	10	0.55	1.3
4	5	12	24	12	0.50	1.6
5	6	20	40	16	0.40	1.9
6	6	25	50	18	0.36	1.9
7	8	42	84	24	0.29	2.6
8	8	49	98	26	0.27	2.6

Notes. n_i, number of edge S atoms at one edge on top plane.

$$L_{max}(\text{hex}) \sim 0.32[2(n_2 - 1) + 1] \quad \text{for } n_2 > n_1$$
$$\sim 0.32[2(n_2 - 1] \quad \text{for } n_2 = n_1.$$

$$L_{max}(\text{rhomb}) \sim 0.32 n_2.$$

Equations: For hex: $n_1 = n_2 = n$. $\text{Mo} = 3(n-1)^2$. $S_T = 2(\text{Mo})$. $S_e = 2[4(n-1)-4]$. For hex: $n_2 > n_1$. $\text{Mo} = n_1(n_2-1)+n_2(n_1-1)+(n_2-1)^2$. $S_T = 2(\text{Mo})$. $S_e = 2(n_1+2n_2-4)$. For rhomb: $n_1 = n_2 = n$. $\text{Mo} = (n-1)^2$. $S_T = 2(\text{Mo})$. $S_e = 4n - 6$. For rhomb: $n_2 > n_1$. $\text{Mo} = (n_1 - 1)(n_2 - 1)$. $S_T = 2(\text{Mo})$. $S_e = 2(n_1 + n_2 - 3)$.

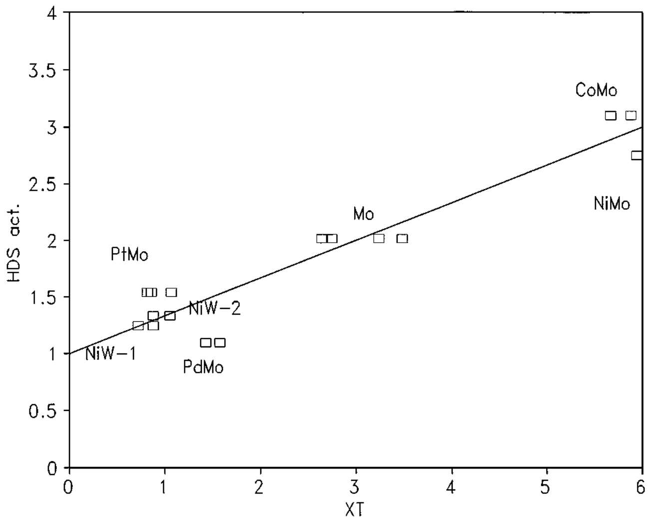

FIG. 2. HDS activity vs total exchange (X_T).

slab size of about 2 nm and contain about 10–15 Mo atoms, again consistent with the EXAFS results.

Another difference in findings occurs when comparing Mo with Co- or Ni-promoted catalysts. EXAFS studies (14, 26, 27) showed little difference, again obtaining ~1.0–1.7 nm for the promoted catalysts. On the other hand, the TEM results (28, 29) showed lower overall sizes for the promoted catalysts compared to the nonpromoted catalyst, but still larger than sizes obtained from EXAFS. Again, our g values of 0.5 ($L \sim 1.3$ nm) and 0.4 ($L \sim 1.6$) for the CoMo and NiMo catalysts agree well with the EXAFS data. We assume the presence of Co (Ni) does not appreciably alter the calculated slab sizes.

Assuming the same argument applies to the NiW catalysts, their lower g would signify much larger slabs (~4 nm). This is in good agreement with TEM results on several sulfided NiW/Al_2O_3 catalysts (28). The Pd/Mo and Pt/Mo catalysts cannot be evaluated due to the presence of separate bulk phases of Pt and Pd containing S (10); the S due to these species (not quantitatively known) would need to be subtracted from the total S to obtain their g values representative of the MoS_2 slabs present. This would increase their g values and decrease their size.

HDS activity is generally associated with vacancies at the edge sites (14). It has been proposed that S exchange is related to vacancies through an adsorption–desorption switch mechanism (2). Hence, a relationship between S exchange and HDS activity might be expected. Such a relationship is shown in Fig. 2, where a fair correlation is seen ($R^2 = 0.90$). Thus, a higher HDS activity is associated with a higher extent of exchange. A similar correlation was obtained by Kogan *et al.* (5) for a series of CoMo catalysts. The surprising feature of the correlation of Fig. 2 is its applicability to a number of different catalysts comprising supported Mo and W formulations.

HDS activity does not relate to the total catalyst sulfur content, as seen in Fig. 3. With the exception of CoMo and NiMo, there is a general lowering in HDS activity with increasing sulfur content for the other catalysts. This is in accord with results reported for Mo/Al_2O_3 catalysts, in which

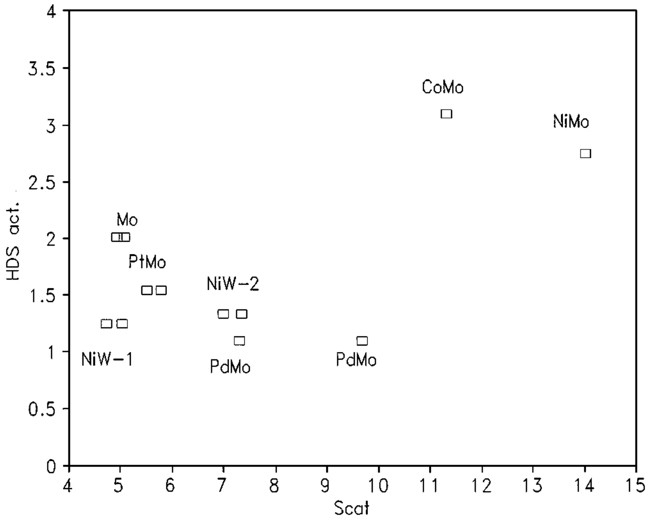

FIG. 3. HDS activity vs extent of sulfiding (S^{cat}).

thiophene HDS activity also decreased with increase in sulfur content above a certain value (30, 31).

CONCLUSIONS

A flow recirculation method, using radioactivity measurements of $H_2{}^{35}S$ during sulfiding and sulfur exchange, was successfully applied to a variety of supported catalysts. Large differences in sulfur uptake and exchangeable sulfur were obtained, depending on the catalyst. The total exchangeable sulfur was considerably less than the total sulfur content of the catalysts. It is proposed that the fraction exchangeable sulfur is related to the edge S to total S ratio. On this basis, average lateral slab sizes were obtained by application of model slabs of MoS_2, and the results were consistent with values found in the literature deduced from EXAFS studies. Catalyst HDS activity correlated reasonably well with the exchangeable sulfur.

REFERENCES

1. Scarpiello, D. A., Montagna, A. A., and Freel, J., *J. Catal.* **96**, 276 (1985).
2. Massoth, F. E., and Zeuthen, P., *J. Catal.* **145**, 216 (1994).
3. Kabe, T., Qian, W., Ogawa, S., and Ishihara, A., *J. Catal.* **143**, 239 (1993).
4. Kabe, T., Qian, W., Tanihata, K., Ishihara, A., and Masazumi, G., *J. Chem. Soc. Faraday Trans.* **93**, 1821 (1997).
5. Kogan, V. M., Greish, A. A., and Isagulyants, G. V., *Catal. Lett.* **6**, 157 (1990).
6. Qian, W., Ishihara, A., Wang, G., Tsuzuki, T., Godo, M., and Kabe, T., *J. Catal.* **170**, 286 (1997).
7. Startsev, A. N., Artamonov, E. V., and Yermakov, Yu. I., *Appl. Catal.* **45**, 183 (1988).
8. Koltai, T., Massoth, F. E., and Tétényi, P., *React. Kinet. Catal. Lett.* **71**, 85 (2000).
9. Koltai, T., Dobrovolszky, M., and Tétényi, P., *Stud. Surf. Sci. Catal.* **127**, 137 (1999).
10. Paál, Z., Koltai, T., Matusek, K., Manoli, J.-M., Potvin, C., Muhler, M., Wild, U., and Tétényi, P., *Phys. Chem. Chem. Phys.* **3**, 1535 (2001).
11. Korányi, T. I., Dobrovolszky, M., Koltai, T., Matusek, K., and Tétényi, P., *Fuel Proc. Tech.* **61**, 55 (1999).
12. Koltai, T., Galsán, V., and Tétényi, P., *React. Kinet. Catal. Lett.* **67**, 391 (1999); **68**, 409 (1999).
13. Dobrovolszky, M., Koltai, M., Paál, Z., and Tétényi, P., *Appl. Catal. A.* **166**, 65 (1998).
14. Topsøe, H., Clausen, B. S., and Massoth, F. E., "Catalysis Science and Technology" (J. R. Anderson and M. Boudart, Eds.), Springer-Verlag, New York, 1996.
15. Kasztelan, S., Toulhoat, H., Grimblot, J., and Bonnelle, J. P., *Appl. Catal.* **13**, 127 (1984).
16. Clausen, B., Topsøe, H., Candia, R., Villadsen, J., Lengeler, B., Als-Nielsen, J., and Christensen, F., *J. Phys. Chem.* **85**, 3868 (1982).
17. Sajkowski, D. J., Miller, J. T., Zajac, G. W., Morrison, T. I., Chen, H., and Fazzini, D. R., *Appl. Catal.* **62**, 205 (1990).
18. Dobrovolszky, M., Paál, Z., and Tétényi, P., *Catal. Today* **9**, 113 (1991).
19. Payen, E., Hubaut, R., Kasztelan, S., Poulet, O., and Grimblot, J., *J. Catal.* **147**, 123 (1994).
20. Pratt, K. C., Sanders, J. V., and Christov, V., *J. Catal.* **124**, 416 (1990).
21. Mauchausse, C., Mozzanega, H., Turlier, P., and Dalmon, J.-A., "Proceedings, 9th International Congress on Catalysis, 1988" (M. J. Phillips and M. Ternan, Eds.), Vol. 2, p. 775.
22. Shimada, H., Matsubayashi, N., Sato, T., Yoshimura, Y., Imamura, M., Kameoka, T., and Nishijima, A., *Catal. Lett.* **20**, 81 (1993).
23. Eijsbouts, S., Heinerman, J. J. L., and Elzerman, H. J. W., *Appl. Catal. A* **105**, 53 (1993).
24. Bouwens, S. M. A. M., Prins, R., de Beer, V. H. J., and Koningsberger, D. C., *J. Phys. Chem.* **94**, 3711 (1990).
25. Lauritsen, J. V., Helveg, S., Laegsgaard, E., Stensgaard, I., Clausen, B. S., Topsøe, H., and Besenbacher, F., *J. Catal.* **197**, 1 (2001).
26. Parham, T. G., and Merrill, R. P., *J. Catal.* **85**, 295 (1984).
27. Sankar, G., Vasudevan, S., and Rao, C. N. R., *J. Phys. Chem.* **91**, 2 (1987).
28. Breysse, M., Cattenot, M., Décamp, T., Frety, R., Gachet, C., Lacroix, M., Bachelier, J., Cornet, D., Duchet, J. C., Lavalley, J. C., Bonnelle, J. P., Grimblot, J., Kasztelan, S., Payen, E., Durand, R., Geneste, P., Moreau, C., Olive, J. L., Engelhard, P., Gueguen, C., and Toulhoat, H., *Am. Chem. Soc., Petrol. Div. Prep.* **32**, 291 (1987).
29. Candia, R., Villadsen, J., Topsøe, N.-Y., Clausen, B. S., and Topsøe, H., *Bull. Soc. Chim. Belg.* **93**, 763 (1984).
30. Massoth, F. E., and Kibby, C. L., *J. Catal.* **47**, 300 (1977).
31. Okamoto, Y., Tomicka, H., Imanaka, T., and Teranshi, S., *J. Catal.* **66**, 93 (1980).